Preprints.org

Article

Assessment of Charge Initiation Techniques Effect on Blast Fragmentation and Environmental Safety: An Application of WipFrag Software

Blessing Olamide Taiwo [*] , Yewuhalashet Fissha [*] , Thomas Palangio , Andrew Palangio , Hajime Ikeda , N.Rao Cheepurupalli , Naseer Muhammad Khan , Adams Abiodun Akinlabi , Oluwaseun Victor Famobuwa , Joshua Oluwaseun Faluyi , Youhei Kawamura

Article

Assessment of Charge Initiation Techniques Effect on Blast Fragmentation and Environmental Safety: An Application of WipFrag Software

Blessing Olamide Taiwo [1,*], Yewuhalashet Fissha [2,3*], Thomas Palangio [4], Andrew Palangio [4], Hajime Ikeda [2],

N.Rao Cheepurupalli [5], Naseer Muhammad Khan [6], Adams Abiodun Akinlabi [1], Oluwaseun Victor Famobuwa [7], Joshua Oluwaseun Faluyi [1]   and Youei Kawamura [8]

[1]   Mining Engineering Department, Federal University of Technology Akure, Nigeria; taiwoblessing199@gmail.com

[2]   Department of Geosciences, Geotechnology and Materials Engineering for Resources, Graduate School of International Resource Sciences, Akita University, Japan; d6521115@s.akita-u.ac.jp; ikeda@gipc.akita-u.ac.jp

[3]   Department of Mining Engineering, Aksum University, Aksum 7080, Tigray, Ethiopia

[4]   Wipware Inc; thomas.palangio@wipware.com; andrew.palangio@wipware.com

[5]   Department of Mining Engineering, Bule Hora University, Ethiopia

[6]   Department of Sustainable Advanced Geomechanical Engineering, Military college of Engineering, National University of Sciences and Technology, Risalpur 232002, Pakistan; nmkhan@mce.nust.edu.pk

[7]   Department of Mining Engineering, West Virginia University, USA; ovf00002@mix.wuv.edu

[8]   Faculty of Engineering, Hokkaido University, Sapporo 0608628, Japan kawamura@eng.hokudai.ac.jp

*   Correspondence: taiwoblessing199@gmail.com, d6521115@s.akita-u.ac.jp

Abstract: Blast charge initiation procedures have a significant impact on both mining safety and production rates. In this study, the inventory benefit of an electric initiation system was investigated to assess its influence on both fragmentation and blast-induced damages. The Wipfrag software's was used to examine the size distribution and productivity of 12 small-scale blasts initiated by both non-electric and electric detonators. All blast rounds was initiated with plain type of electric and NONEL detonators. The average burden, spacing, stemming length, and charge weight were, respectively, 0.85 m, 1.10 m, 0.66m, and 1.1kg. The results showed that the mesh through which 80% of the blast fragments will pass for the electric blast is smaller than the mesh through which the material products from the NONEL blast will pass. The results also demonstrate that the generated blast-induced ground vibration (PPV) from all blast rounds for electric blast varies from 0.4–1.2 mm/s and 80–105dB, while that for non-electric blast ranges from 0.05–0.2mm/s and 72–95dB. As a result, the electric blast initiation technique was found to produce good fragmentation, with a higher percentage of optimum fragment sizes on spec than non-electrically initiated blasts.

Keywords: marble; small-scale mining; blast impact; fragments size characterization; WipFrag,

1. Introduction

Marble is a type of granular limestone or dolomite that has been recrystallized by heat, pressure, and aqueous solutions [1]. Marble is a coarse industrial rock element with a high carbonate content that varies in occurrence; it is widely used in the cement and paint industries [2]. Marble occurs in a wide range of geological environments, including mountain ranges, fault zones, and sedimentary basins [3]. Some of the most famous marble quarries in the world are in Italy, Greece, and Turkey, where the stone has been cherished for ages for its beauty and durability [4]. These countries have both large-scale and small-scale marble mines, which contribute to their GDP due to the widespread industrial use of marble powder and rock aggregates. Egypt has the highest volume of marble construction stone output, accounting for 93% of the total volume. Zambia came in second,

accounting for 2.3% of total production. African countries, such as South Africa, have also been involved in large-scale marble block manufacture. Nigeria is endowed with huge reserves of limestone and marble throughout the country. The limestone in Mfamosing, near Calabar, is Nigeria's largest and purest deposit. The rate of marble production in Nigeria is determined by the mining process and the rate of output. The majority of Nigeria marble is fragmented using blasting procedures. Small-scale marble production, unlike large-scale mines with varied expert opinions and research inputs, requires innovation to increase safety and productivity. The ever-increasing need for industrial minerals like carbonate material for cement and paint production in Nigeria has prompted the creation and management of both small-scale and large-scale quarries. According to [6] artisanal and small-scale mining (ASM) is mineral extraction by individuals, cooperatives, or small businesses with little financial investment and a heavy reliance on physical labour. According to Warra and Prasad, ASM has been identified as one of the most important economic activities in many rural communities in Sub-Saharan Africa. According to their findings, small-scale mining operations in Nigeria are expanding in intensity. The use of explosives to reduce rock mass can have a number of negative effects on the environment, mine workers, and major human health issues [8]. Artisanal mining in Nigeria, particularly in its southwestern section, is said to be at best unplanned and haphazard, with significant environmental consequences [7,9]. In mining, blasting operations are routinely employed to break up in-situ rock masses in order to ensure material availability [10,11]. The fundamental purpose of blasting activities, according to Jhanwar, is to generate enough energetic wave energy for rock mass fracturing and size reduction [12]. The quantity of explosive energy during detonation is measured in a number of ways, including computations and experimental experiments. However, it is unclear how much of that explosive energy is delivered to the rock for fragmentation and how much of it is transformed into efficient work in the typical mining use of rock blasting. Although some of the effects of explosive excess energy utilisation have been explained as vibration, fragmentation, and rock displacement, these measurements are normally done for blast control purposes, and the results are usually important to guarantee a sustainable blasting environment. Blasting procedures are less productive when fine and boulder fragments are produced [13]. According to [14–16], a rise in fine fragment sizes in blast results influences the production rate as well as the effectiveness of loading and downstream activities. According to Jethro et al., the presence of stones in blast muck has a negative impact on haulage and raises the cost of loading, transporting, and subsequent run-off-mine processing [17].

Overall, when the after-effects of blasting operations are adjusted, the cost and effectiveness of comminution operations (crushing and granulating) will be enhanced. For a long time, mining engineers had hoped that improving blasting fragmentation results would lead to increased productivity. The use of empirical and soft computing models in estimating blasting production and blast-induced consequences is possibly the most important aspect in this anticipation. These blast-induced consequences are caused by the unused energy released upon explosion and contribute to the mine's significant environmental issues. Ground shock and vibration are caused by rock blasting, which can harm neighbouring structures [18]. Because of the rising hazard posed by diverse man-made activities, the reduction of blast-induced effects on natural and man-made buildings has garnered a lot of attention in recent decades [19]. Nonetheless, small-scale mining sectors continue to dominate in terms of environmental effect generation. As small-scale mines become closer to human habitation, it is critical to conduct out blasts with safer initiating methods in order to limit ground vibrations and noise while maintaining a high output rate. Manufacturers commonly claim that the non-electric shock tube system (NONEL) improves all blasting results for large-hole blasting while leaving no trace of small-scale blasting.

The utilization of Jackhammer small hole diameter blasting with candle type explosive for blasting at small scale extraction level is applicable to both industrial and metallic mineral extraction. This is commonly used in small scale mines for primary blasting and in large scale mines for secondary blasting operation. To understand the effect of charge initiation techniques on small hole diameter blasting, this study examine the safety and production rate of electric and non-electric detonation process in   small scale mine at Akoko Edo, Nigeria.

3

2. Materials and Methods

This section explains the methodology used in achieving the purpose of this study, and also gives brief information about the mine's geological properties and mine site state of art condition.

The case study mine, a small-scale quarry in Akoko Edo, Edo state, Nigeria, is loacated in Akoko Edo, Nigeria as presents in Figure 1. The Wipware sample guide version 1 approach was used to acquire fragmentation images from 12 production blast rounds for size distribution analysis using WipFrag version 3.3. After blasting and mid-loading operation time blast images were captured with a camera totally with the necessary scaling object as specified by the Wipware sample guide (see Figure 2). Figure 3 depicts the flow sheet/specific objectives of this research project.

The quarry blast report provided blast design characteristics such as burden, spacing, drill hole length, hole diameter, and stemming for 12 blast rounds. According to the quarry blast design that was observed, the drill pattern utilised in the mine was identified as staggered. Twelve blast rounds were used in this investigation to assess the performance of electric and non-electric blast initiation production. [23] proposed a non-electric detonator as a flexible tube made of plastic with a diameter of 3 mm. The nonel detonator (cap) employed has a VOD of 2000 m/s. The electric detonator is made up of a thin plate with a thickness of 0.3 mm and a copper or aluminium tube with a diameter of 6 mm and a length of 32 to 53 mm [23]. The detonator tube is made up of a base charge and a prime charge; the main charge includes the detonating medium, pentaerythritol tetranitrate (PETN). The lead azide, lead styphnate, and a trace of aluminium powder known as ASA are all present in the prime charge [23,24]. In this study, plain electric and NONEL detonators were used for six explosion rounds each.
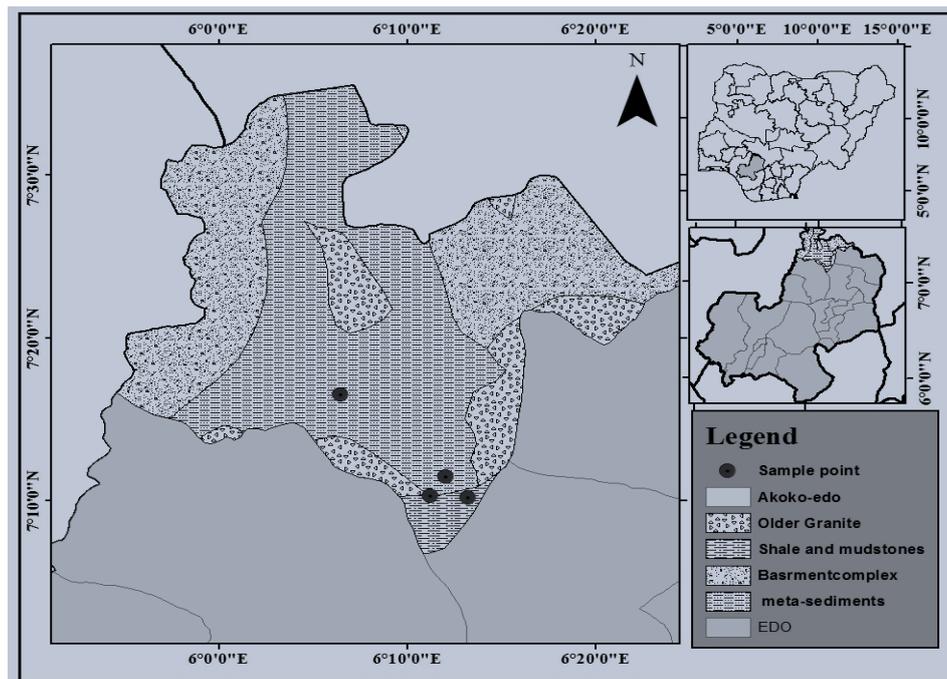

Figure 1. Topographic map of Ikpeshi Akoko Edo showing the case study area.

(a)   (b)
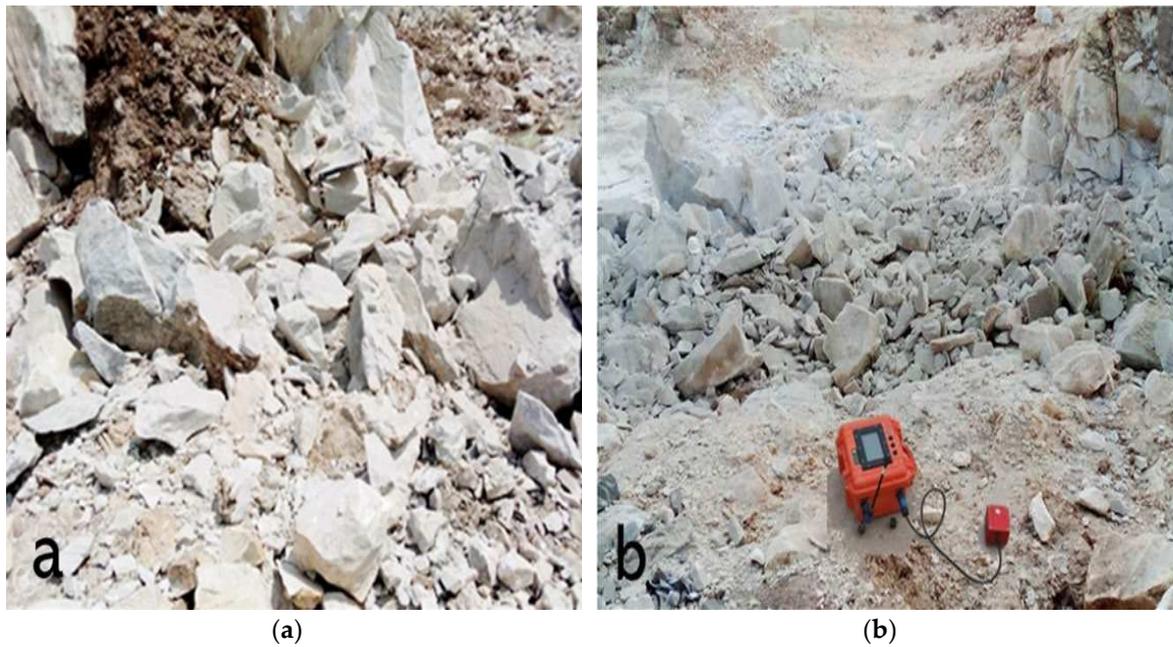
Figure 2. Marble fragmentation pile (a) and pile with PPV measure device (b).

The impact of the initiation method on fragmentation results, blast-induced vibration, and noise levels generated was investigated. Table 1 provides a summary of the quarry blast design parameters. The average burden, spacing, stemming length, and charge weight were, respectively, 0.85 m, 1.10 m, 0.66 m, and 1.1 kg. The typical stiffness ratio is 1.6, and the mine blast power factor ranges from 0.6 to 1.0 kg/m3. The bottom charge material in the case study mine is Dynogel explosive, and the hole column charge material is ammonium nitrate fuel oil (ANFO).
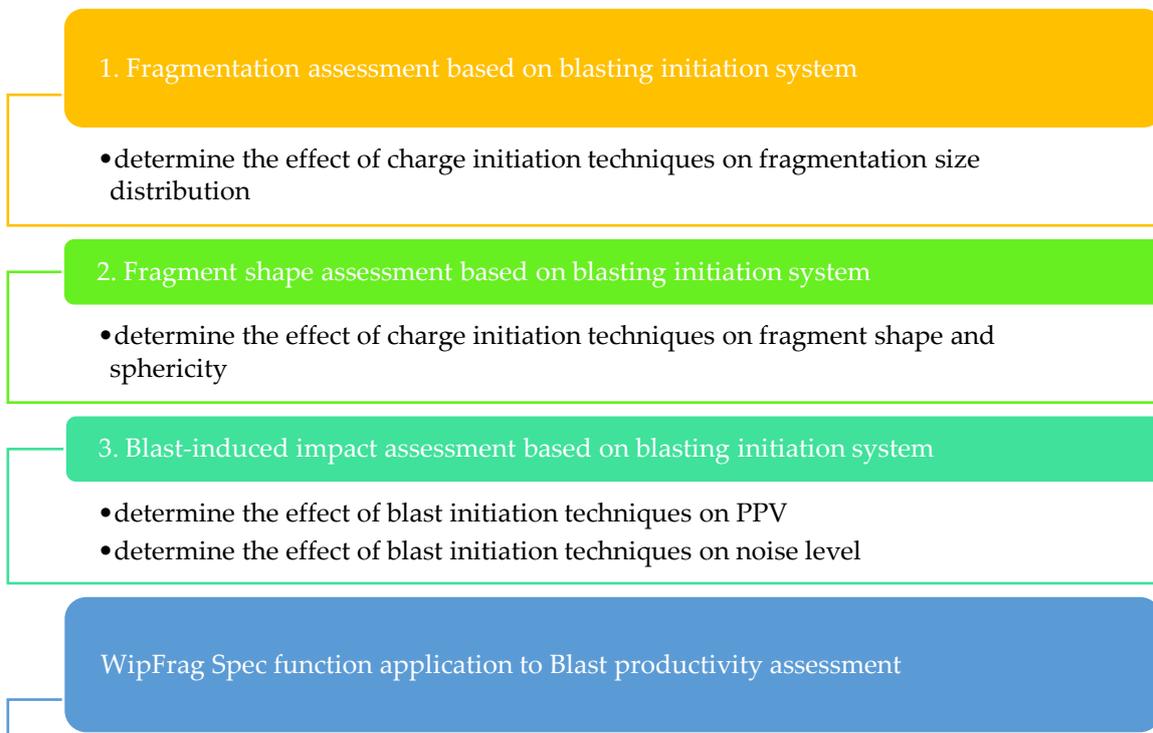
Figure 3. The summary of the Study objectives.

Table 1. Blast Design Parameters for the case study quarry.

Blast Parameter	Average value

Burden (m)	0.85
Spacing (m)	1.10
Hole Depth (m)	1.35
Drill pattern	Staggered
Hole Diameter (m)	0.04
Drill Hole Depth (m)	1.35
Stemming (m)	0.66
Sub drill (m)	0
Charge length (m)	0.65
Charge weight (kg)	1.1

WipFrag 3.3 software was used to perform fragmentation analysis on the blasted material after each blast round. As [25] points out, fragmentation analysis allows for the determination of rock size and the distribution of particle sizes. WipFrag is an image inspection framework used to size materials such as blasted or crushed stone heaps. WipFrag, according to Maerz, is a cutting-edge image-based granulometry solution built particularly for high-contrast graytone images [26]. In mining operations, Digital Image Analysis Technology (DIAT) provides an automated system that estimates material size distribution, resulting in cost savings and reduced damage caused by excessive materials. WipWare Inc. is a Canadian firm that specialises in image analysis software and technology for the mining, aggregate, and related industries. Tom Palangio launched the company in 1995, seeing a need for automated image analysis technologies in the mining industry. Wipware's main product is the WipFrag programme, which analyses the size distribution of fragmented particles in a rock mass using digital image processing. Wipfrag is a Solo System software package designed to analyse the size distribution of fragmented particles in a rock mass [27]. In the mining industry, Wipfrag is extensively used to examine the size distribution of blasted rock pieces in order to optimise drilling and blasting operations [28,29].

To evaluate photos of fragmented particles, the software uses a technique known as digital image processing [30]. The user uploads a snapshot of the rock pile or muck pile into the software. The software then recognises and measures the size of each particle in the image automatically. Wipfrag provides a size distribution graph of the particles, which may be used to calculate the average size of the fragments, maximum and lowest sizes, and size distribution uniformity. In this work, Wipfrag version 3.3 was utilised to evaluate the influence of both electric and non-electric initiation mechanisms on fragmentation shape and size distribution. A systematic sampling technique was used in this work to avoid the difficulty of material proportion oversight. Each blast round with a known-size scaling item yielded many images. The size distribution assessment took into account both the first material spread after blasting and the loading advancement image (see Table 2).

Table 2. Assigned blast identification number for each captured image.

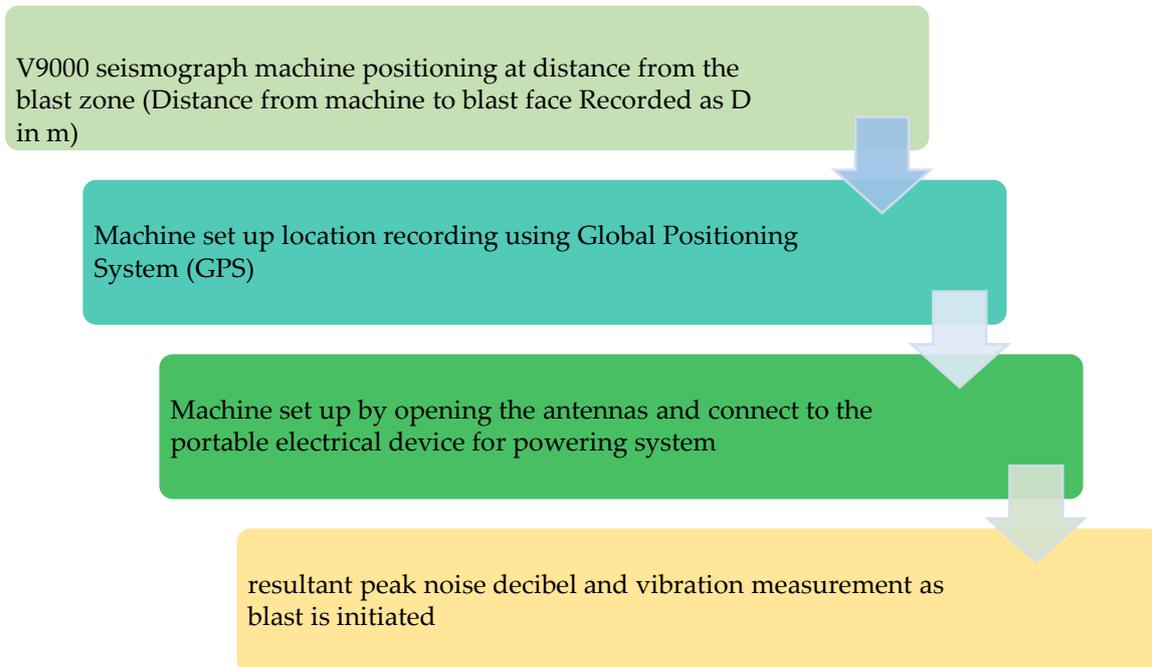| Blast ID	Description
BL1-1	Image from blast round one after blasting before loading
BL 1-2	Image from blast round one after loading advancement
BL 2-1	Image from blast round two after blasting before loading
BL 2-2	Image from blast round two after loading advancement
BL 3-1	Image from blast round three after blasting before loading
BL 3-2	Image from blast round three after loading advancement
BL1-1: blast 1 at pit 1, BL 1-2: blast 1-2 at pit 1, BL2-1: blast 1 at pit 2, BL 2-2: blast 2 at pit 2, BL3-1: blast 1 at pit 3, BL 3-2: blast 2 at pit 3	

The procedure for the measurement of the generated noise level and vibration is presented in Figure 4. Adopting the [31] analysis method, information on blasting activities was used to compile values of scaled distance for each recorded seismograph reading, using distance to the nearest recording seismograph. Scaled distance is defined herein as the distance from the blast to the recording seismograph, D, divided by the square root of the maximum weight of explosives

detonated per 8-millisecond delay window, W, in kg. The results generated were interpreted and presented quantitatively and qualitatively in Section 3. The scaled distance equation suggested mostly for cylindrical charge in the literature was used for the prediction of peak particle velocity (PPV) as presented in Equation 1 [32].

$$SD = \frac{D}{\sqrt{W}}$$

(1)

Where SD is the scaled distance in $m/kg^{0.5}$, D is the measuring equipment distance in m, and W is the total explosive weight (kg).

V9000 seismograph machine positioning at distance from the blast zone (Distance from machine to blast face Recorded as D in m)

Machine set up location recording using Global Positioning System (GPS)

Machine set up by opening the antennas and connect to the portable electrical device for powering system

resultant peak noise decibel and vibration measurement as blast is initiated

**Figure 4.** Ground vibration and noise level measurement proceures.

3. Results

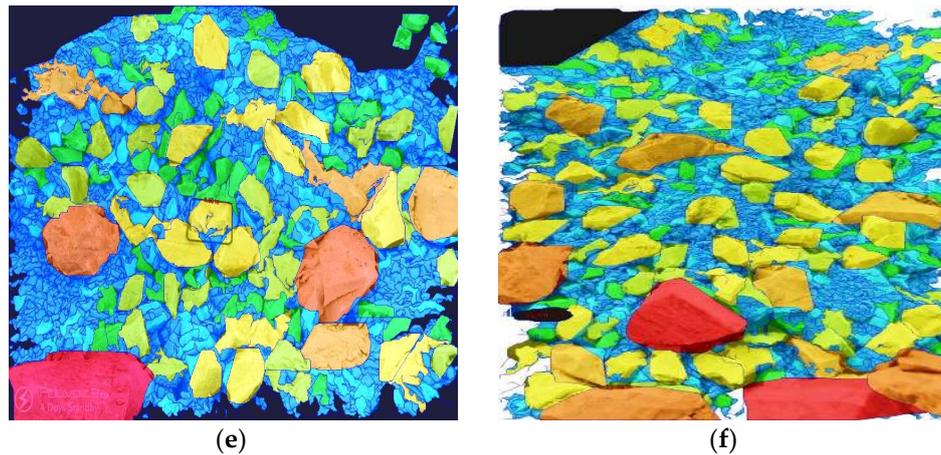### 1.3.1. Fragmentation analysis Results

The fragmentation results for both electric and NONEL blast rounds were determined and compared to assess the effect of blast initiation on fragmentation size. The imag analysis results for electric and non electric blast rounds are presented in Figures 5-6 respectively. The Wipfrag 3.3 specification function used as downstream operation efficiency assessment was implemented in this study to consider the case company size distribution result expectation. The mesh sizes greater than 316 mm were tagged oversize, and the spec was within 0 to 20% retention rate. The mesh sizes less than 20 mm were tagged undersize and spec within 0 to 20% grain passing rate. The optimum size range was set within 147–316 mm at 70%–100% spec range.

(**a**)   (**b**)

(c)

(d)

(e)

(f)
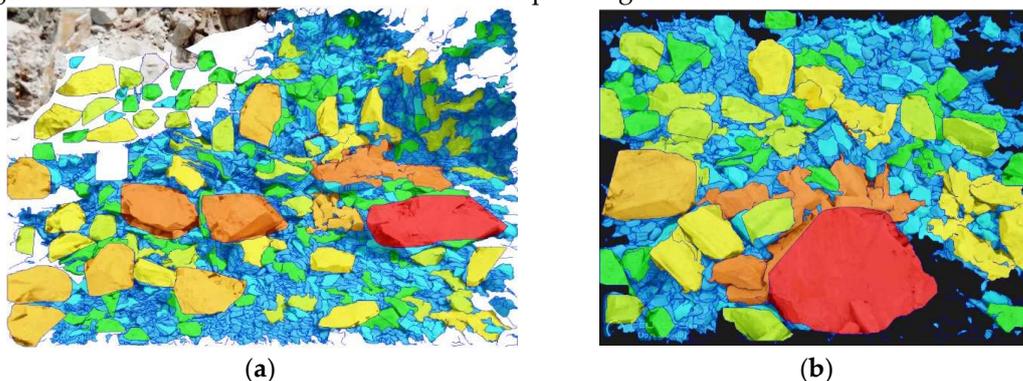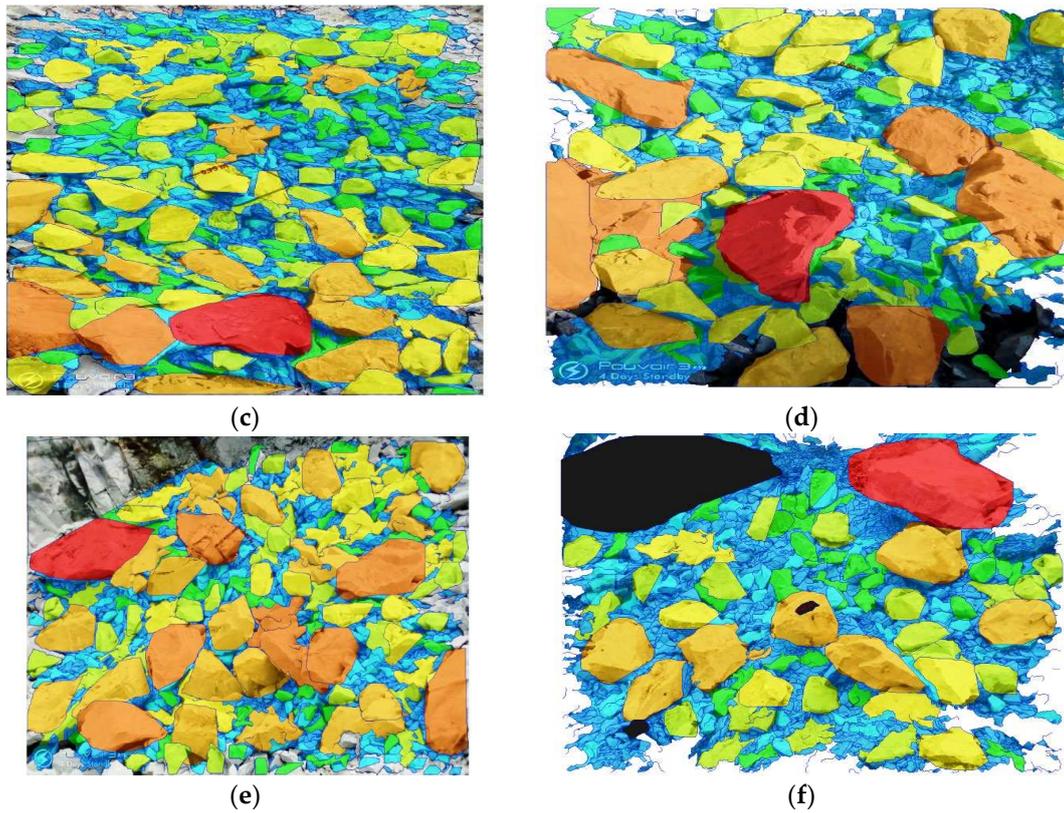
Figure 5. NONEL Blast result image analysis (Result from WipFrag 3.3 edge detection process); a. Blast 1-1, b. Blast 1-2, c. Blast 2-1, d. Blast 2-2, Blast 3-1, and Blast 3-2.


(a)

(b)

(c)

(d)

(e)   **(f)**
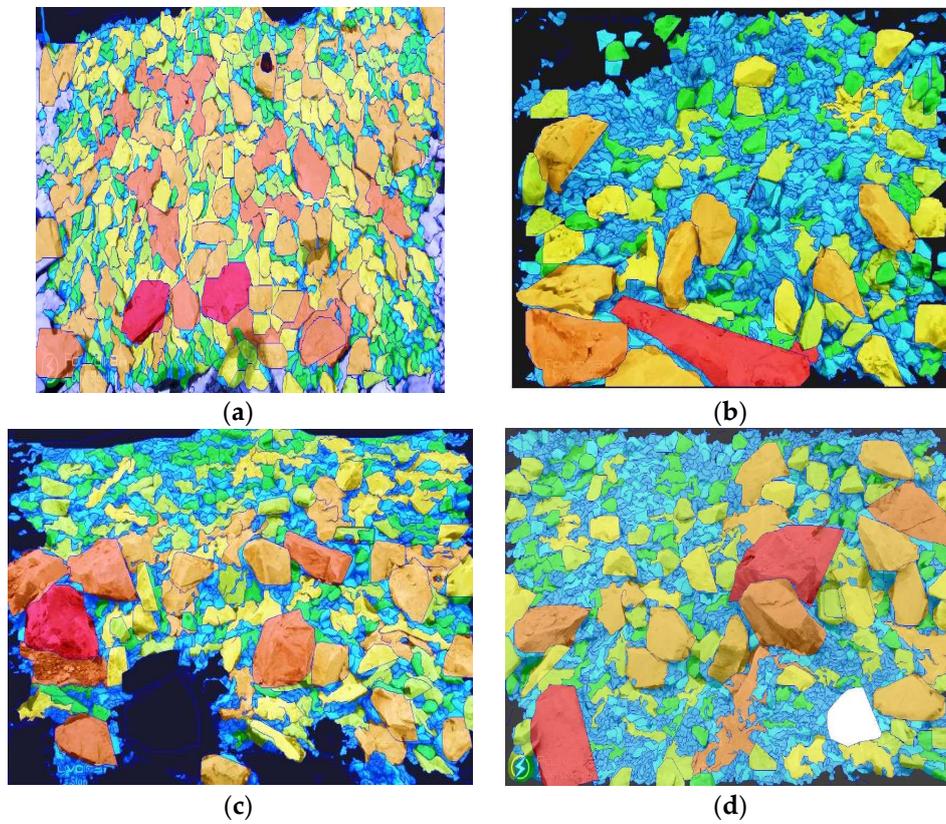
Figure 6. Electric Blast result image analysis (Result from WipFrag 3.3edge detection process); a. Blast 1-1, b. Blast 1-2, c. Blast 2-1, d. Blast 2-2, Blast 3-1, and Blast 3-2.

1.3.1. Fragmentation result for NONEL blasting

Figure 7 presents the fragmentation size distribution obtained from the six nonelectric blasting results analysed using Wipfrag 3.3 software. The result, as shown in the cumulative curves, has bigger boulders with sizes ranging from 735 mm to 1179.47 mm for the 80% passing size (X_{80}).
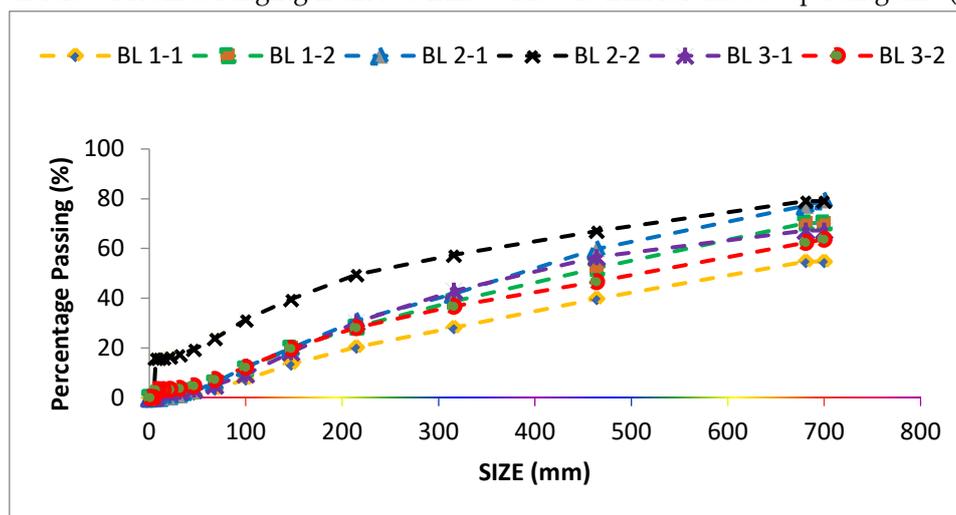
Figure 7. Fragmentation Analysis result for NONEL Detonator.

1.3.2. Fragmentation result for electric blasting

The fragmentation analysis for the electric blast round result is illustrated by Figure 8. The mean size ($X50$) for blast 1-1, blast 1-2, blast 2-1, blast 2-2, blast 3-1, and blast 3-2 are 462.25 mm, 328.53 mm, 258.14 mm, 336.11 mm, 235.62 mm, and 120.52 mm, respectively.
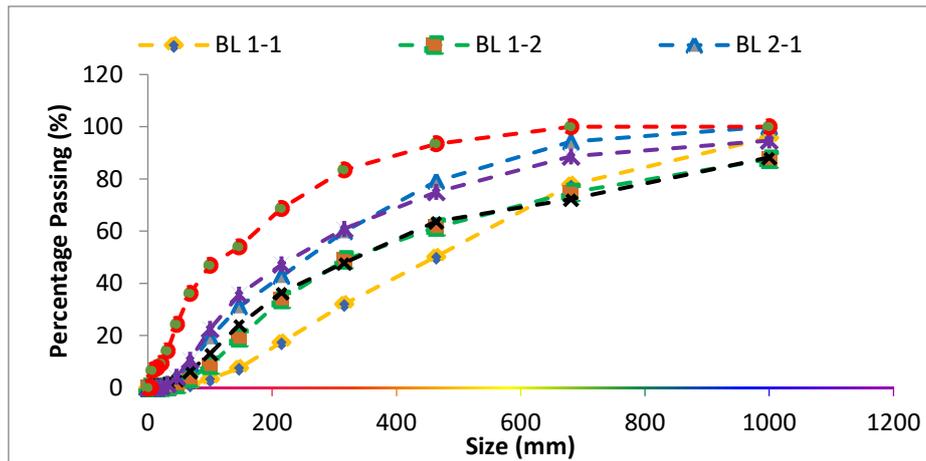
Figure 8. Fragmentation Analysis result for electric Detonator.

1.3.3. Fragmentation assessment results

Utilising additional Wipware photo analysis software features, the efficacy of the two blast initiation techniques was further evaluated. The Wipfrag analysis yields both particle distribution curves and additional evaluation parameters. Image analysis sphericity is the average ratio of the largest dimension to the longest perpendicular dimension of each particle. For instance, a Wipfrag result of 0.5sphericity suggests that the average particle in the blast pile is twice as long as it is broad. Non-electric blast provides the greatest sphericity sizes for the highest blast rounds, as demonstrated by the result. The sphericity of explosion fragments from both electric and non-electric blast rounds is depicted in Figure 9a. Figures 9b and 9c display the average particle size and 80% passage size for both electric and non-electric blasts, as determined by the WipFrag 3.3 software.

(a)

(b)
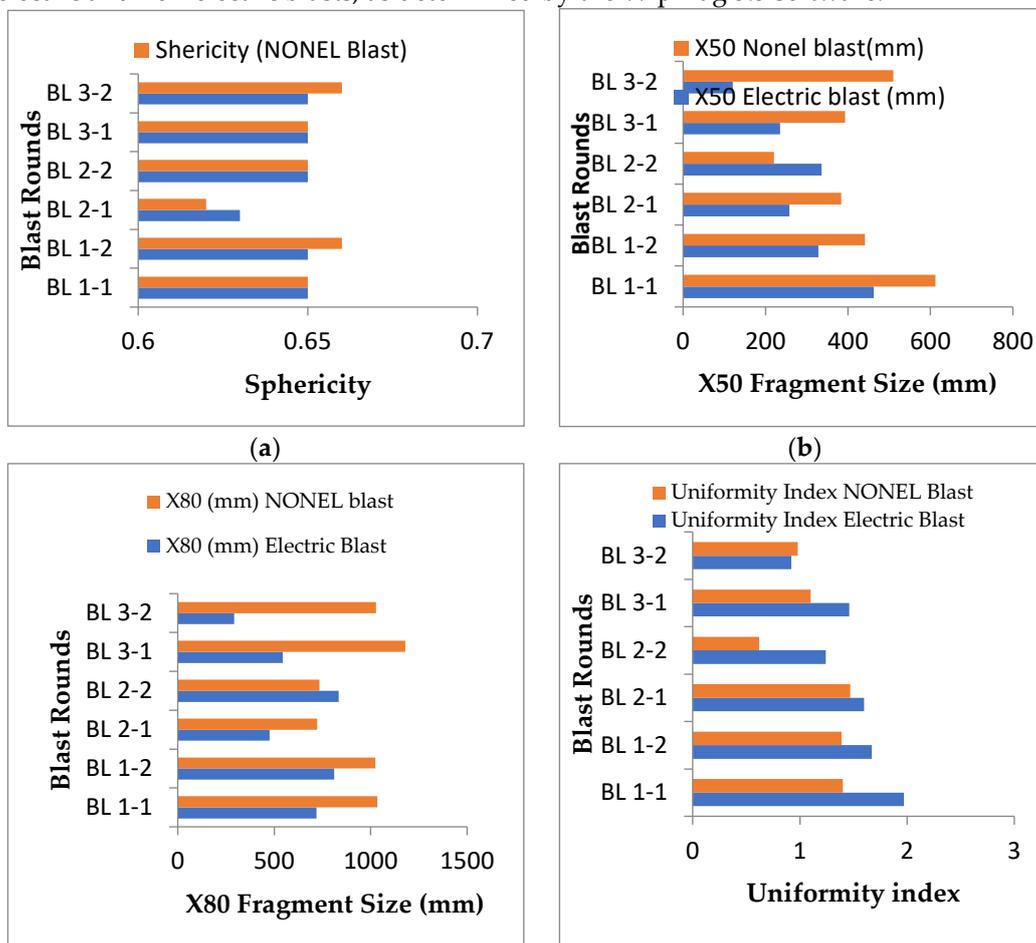
(**c**)   (**d**)

Figure 9. Comparison between Non Electric and electric blast using Wipfrag 3.3 analysis output; a. sphericity results, b. X50 results, c. X80 results, and d. uniformity index results.

The fragmentation result seems not to be sufficient for decision-making due to other factors different from production assessment. Most importantly, the safety of the mine, nearby structures, and mine equipment requires considerate assessment. The results of the structural and environmental impacts of both initiation techniques are presented and discussed in the next section.

1.3.4. Blast-induced impact result

Blasting operations have been cognizant of blast impacts on the environment, mine personnel, and equipment for decades [37–40]. In addition to facilitating the separation of mineral fragments from rock masses, blasting operations contribute to a variety of other environmental maladies, such as ground vibration, backbreak, noise pollution, and dust dispersion. This section compares the effectiveness of electric and non-electric detonators based on the impact generated by six explosion rounds. The average ground vibration and noise level for the non-electric blasting rounds are 0.108 mm/s and 81.7 dB, respectively. The average ground vibration and decibel level for the six monitored electric blasting rounds were 0.76 mm/s and 92.5 dB, respectively. The results indicate that the blast-induced ground vibration (PPV) generated by all of the blast rounds for electric blast ranges from 0.4–1.2 mm/s and 80–105 dB, while that of the non-electric blast round ranges from 0.05–0.2 mm/s and 72–95 dB.

3.4.1. Comparison between the two initiation techniques

The comparison between the blast-induced ground vibration and decibel level from electric and non-electric blasting rounds is depicted in Figures 10 and 11. In comparison to non-electric detonators, the decibel levels and ground vibrations during electric blasting are greater than that of the non electric blasting rounds.
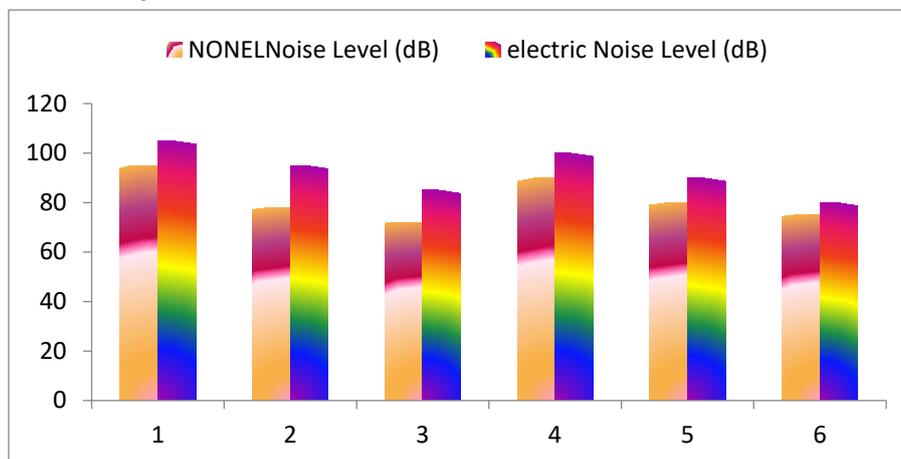
Figure 10. Comparing blast induced Noise level from both electric and NONEL initiated blast.
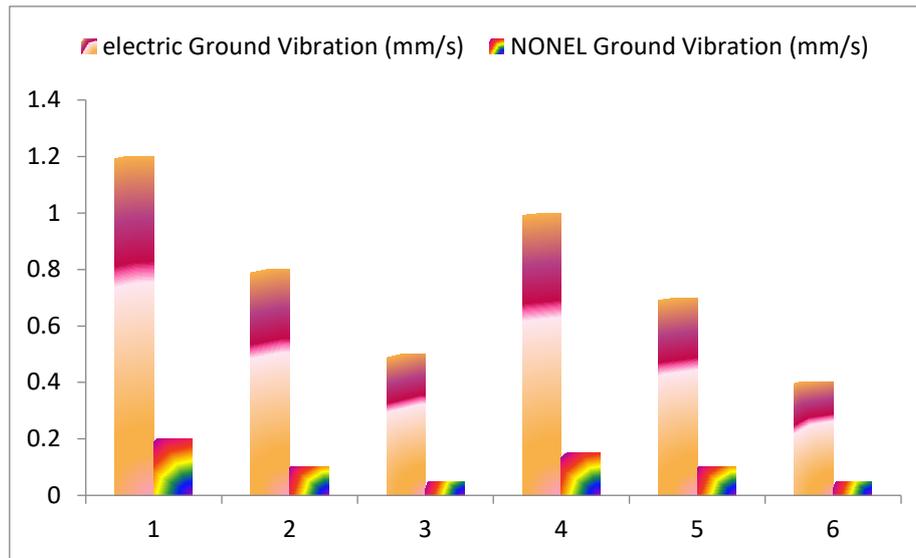
**Figure 11.** Comparing blast induce ground vibration from both electric and NONEL initiated blast.

3.4.2. Regression Model for Blast impact Prediction

Figures 12 and 13 show the relationship between scale distance, ground vibration (PPV) impact, and noise level of the blasting operation at the case study mine. Ground vibration variability with scaled distance was revealed to have a negative correlation. The peak particle velocity and noise level values decrease as the scaled distance increases, supporting existing works [42–44]. The combined results from all the study blast experiments were used to develop a logarithmic model for predicting ground vibration and noise level using the scale distance as the input variable. The developed logarithmic model is presented in Equations 1 and 2. The model result shows good prediction accuracy with a high correlation coefficient (R^2) of 0.854 for ground vibration and 0.647 for noise level estimation.
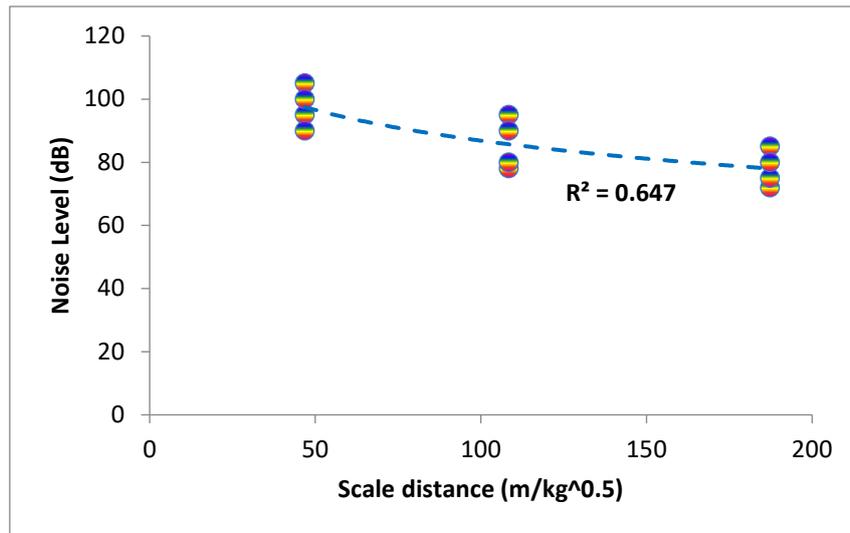
$$PPV = -0.62\ln(SD) + 3.295 \tag{2}$$
$$NL = -14.0\ln(SD) + 151.6 \tag{3}$$

Where PPV is the peak particle velocity mm/s, SD is the scale distance in $m/kg^{0.5}$, NL is the noise level in dB.
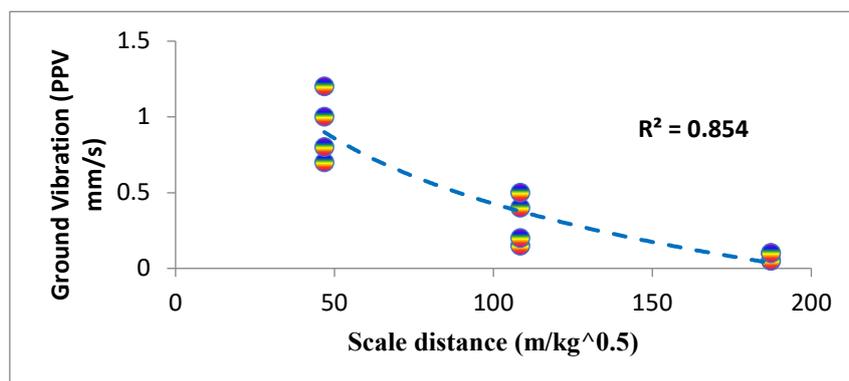
**Figure 12.** Relationship between Ground Vibration and Scale distance.

**Figure 13.** Relationship between Noise level and Scale distance.

1.3.5. Wipfrag software Spec function and Chart Size Classifier results

This section presents the application of the Wipfrag software specification function (Spec) as a tool for fragmentation efficiency assessment based on the primary crusher inlet size. The sieve size was adjusted for a low percentage passing range for fine material less than 30 mm and a large percentage passing range for the optimum size between 215 mm and 464 mm gape. The oversize gape (>464 mm) was specified at the maximum passing size.

3.5.1. Non Electric blast result production assessment

The six blast rounds from the non-electric blasting were assessed using the Wipfrag 3.3 spec adjustment function. The yellow boundary demonstrates the projected maximum trend for the blast particle size distribution curves. The results of the non-electric blast have a lower percentage on-spec result, as shown in Figure 14. All the non-electric blast round results were revealed as off-spec for 316 mm and 215 mm sieves. The result implication is that the percentage of rock fragments passing through 316 mm and 215 mm mesh is lower than the 70% minimum bench mark set for all the non-electric blast results. Furthermore, as for all the experiment blast outputs, the primary inlet size material falls below the production-efficient spec area.

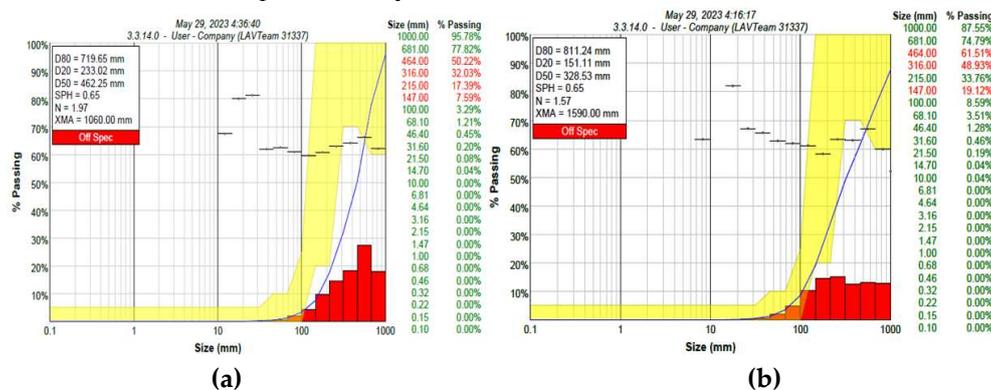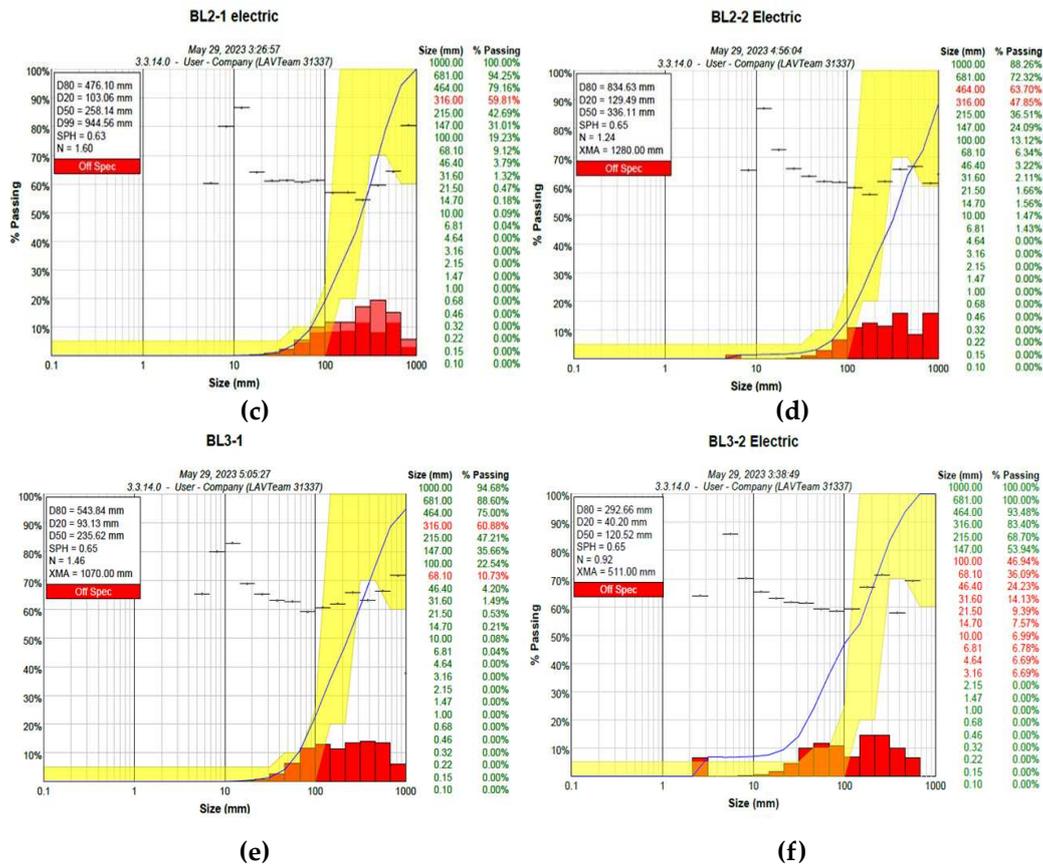(a)   (b)
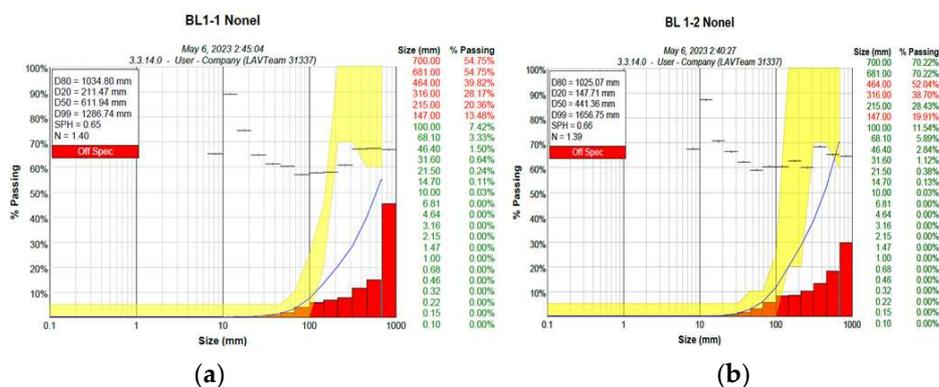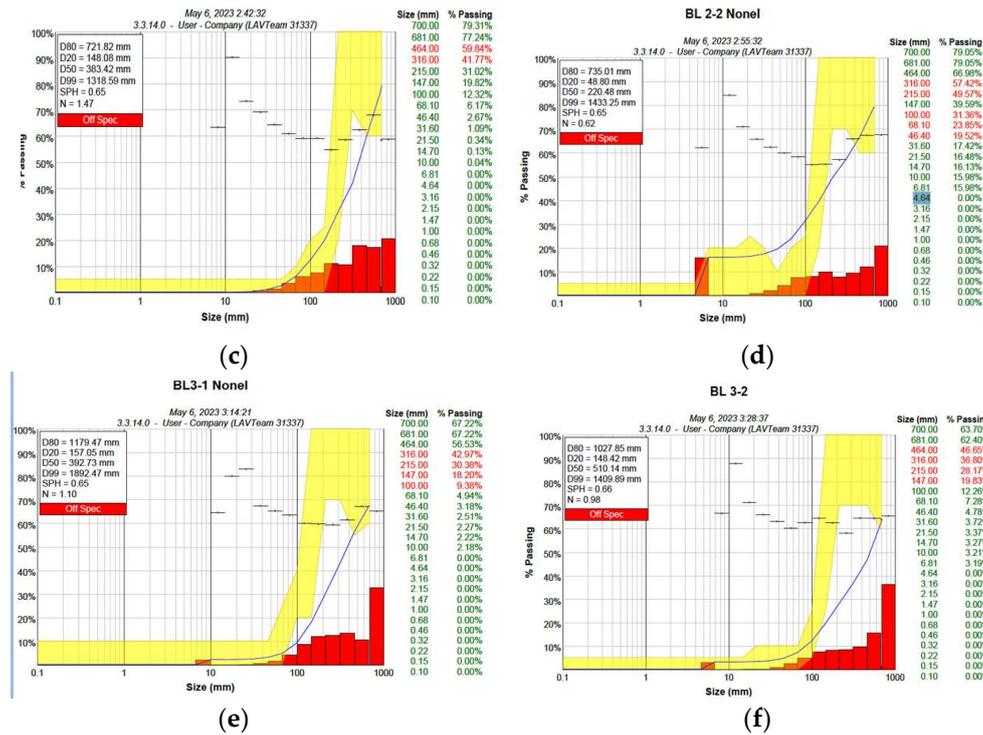
Figure 14. WipFrag Spec function cumulative curve for Non Electric blast rounds; (a) Blast 1-1, (b) Blast 1-2, (c) Blast 2-1, (d) Blast 2-2, (e) Blast 3-1, and (f) Blast 3-2.

3.5.2. Electric blast result production assessment

The electric blast results have a higher percentage of spec results, as shown in Figure 15. 80 percent of the electric blast round results were revealed to be on spec for 316 mm and 215 mm sieves. The result implication is that the percentage of rock fragments passing through 316 mm and 215 mm mesh is greater than 70%, the minimum bench mark set for all the electric blast results. Furthermore, as for all the experiment blast outputs, the primary inlet size material falls within the production efficiency spec area. As such, the electric blast initiation technique was found to have generated good fragmentation, with a larger percentage of optimum fragment sizes on spec than those produced by a non-electric blast.

Figure 15. WipFrag Spec function cumulative curve for Non Electric blast rounds; (a) Blast 1-1, (b) Blast 1-2, (c) Blast 2-1, (d) Blast 2-2, (e) Blast 3-1, and (f) Blast 3-2.

4. Discussion

In general, all the blast rounds show high passing efficiency, with sieve sizes ranging from 600 mm to 1000 mm. The mean size (X_{50}) for blast 1-1, blast 1-2, blast 2-1, blast 2-2, blast 3-1, and blast 3-2 are 611.94 mm, 441.36 mm, 383.42 mm, 220.48 mm, 392.73 mm, and 510.14 mm, respectively. Blast rounds for the same design (blast 1-1 and blast 1-2), blast 2-1 and 2-2, and blast 3-1 and blast 3-2) gave different results, indicating the effect of rock intrinsic properties. This shows that blasting results do not only depend on the initiation method but also on the intrinsic properties of the rock, as mentioned in several findings [33–35]. This finding also revealed that non-electric detonation techniques performed poorly with low percentage optimum size material as specified by the company's primary crusher inlet size (350 mm by 420 mm).

This finding also revealed that electric detonation techniques performed better with higher percentages of optimum size material as specified by the company's primary crusher inlet size (350 mm by 420 mm). As compared to the results of the non-electric blasting, it was revealed that the electric blasting techniques give a high percentage of small-size materials (see the horseshoe trend in Figure 8), as also mentioned in Cardu et al.'s [36] review work.

The illustration of the results demonstrates that the average particle sizes of non-electric explosion fragments are larger than those of electric blast fragments. This demonstrates that electric blast techniques produce superior fragmentation results compared to NONEL blast techniques. The outcome indicated that the mesh size through which 80% of the explosion fragments will pass for the electric blast is smaller than that for the NONEL blast. As depicted in Figure 9d, the Rosin-Rammler uniformity coefficient result for both blast initiation procedures is compared. The WipFrag software result indicates that, for more than 80 percent of the blast rounds, the fragmentation produced by electric blasting is more uniform than that of the NONEL blast material.

According to the measured ground vibration, noise level, and scale distance for six non-electric blasting rounds, it was noted that the blast-induced ground vibration (PPV) generated by all of the

blast rounds for electric blast ranges from 0.4–1.2 mm/s and 80–105 dB, while that of the non-electric blast round ranges from 0.05–0.2 mm/s and 72–95 dB. Based on [41] findings, the results from both initiation techniques at the small scale mine are lower than the values measured at the Ewekoro limestone mine. In addition, the average value of all experimental explosions was found to be below the Federal Environmental Protection Agency's safety threshold.

The comparison between the blast-induced ground vibration and decibel level from electric and non-electric blasting rounds is depicted in Figure 10 and 11. In comparison to non-electric detonators, the decibel levels and ground vibrations during electric blasting are greater. According to [23], this result was attributed to the simultaneous occurrence of the instantiated discharge command effect. High instantaneous initiation from the electric detonator has been observed to support the release of high explosive pressure from the blast charge, which contributes to the generation of large-magnitude waves [42].

5. Conclusions

The present study has been carried out to assess the effect of electric and non-electric initiation techniques on blast production and blast-induced impact generation. The present research also demonstrates the application of Wipfrag's spec function and spec outline chart in assessing blast production efficiency. From the overall analysis, the following conclusions are drawn:

The study result revealed that electric detonation produces high percentages of fines as compared to the Wipfrag analysis result from non-electric detonator blasting.

The finding revealed that electric detonation techniques generate high percentages of optimum size material for 80% of the overall blast rounds as compared to the company's primary crusher inlet size range (316 mm and 215 mm mesh).

The results show that the generated blast-induced ground vibration (PPV) from the electric blast ranges from 0.4–1.2 mm/s and 80–105 dB, respectively, and also from 0.05–0.2 mm/s and 72–95 dB for the non-electric blast.

The result reveals that the noise levels and ground vibrations are higher in electric blasting compared to non-electric detonator blasting. Ground vibration variability with scaled distance was revealed to have a negative correlation. Also, the peak particle velocity and noise level were revealed to decrease as the scaled distance increased.

The Wipfrag spec function indicates that 80% of the electric blast round results were on spec for 316 mm and 215 mm sieves, with mesh passing greater than 70% of the minimum bench mark set for all blast results.

The author's future work will focus on applying the deep learning algorithm in Wipfrag 4.0 to simulate more blast image analysis for better assessment. Moreover, the authors also plan to utilise the orthomosaic features in the new version to capture underlying particles and more fine materials in the muck pile.

References

1. Le Bas, M. J.; Spiro, B.; Xueming, Y. Oxygen, carbon and strontium isotope study of the Carbonatitic dolomite host of the Bayan Obo Fe-Nb-REE deposit, Inner Mongolia, N China. *Mineralogical Magazine*, 1997; *Volume* 407, pp.531-541.
2. Taiwo, B. O.; Omotehinse, A. O. The economic potential of some metacarbonate rocks in Akoko-Edo, Edo state Nigeria. *Applied Earth Science*, 2022; Volume 3, pp.167-178.
3. Dzikowski, T. J.; Cempírek, J.; Groat, L. A.; Dipple, G. M.; Giuliani, G. Origin of gem corundum in calcite marble: The Revelstoke occurrence in the Canadian Cordillera of British Columbia. *Lithos*, 2014; pp.281-297.
4. Winkler, E. *Stone in architecture: properties, durability*. Springer Science & Business Media, 1997.
5. Pitra, P.; De Waal, S. A. High-temperature, low-pressure metamorphism and development of prograde symplectites, Marble Hall Fragment, Bushveld Complex (South Africa). *Journal of Metamorphic Geology*, 2001; *Volume* 3, pp.311-325.
6. Hilson, G. Formalization bubbles: a blueprint for sustainable artisanal and small-scale mining (ASM) in sub-Saharan Africa. *The Extractive Industries and Society*, 2020; *7*(4), pp.1624-1638.
7. Warra, A. A.; Prasad, M. N. Artisanal and small-scale gold mining waste rehabilitation with energy crops and native flora—a case study from Nigeria. In *Bio-geotechnologies for mine site rehabilitation*, 2018; pp. 473-491.
8. Zhu, F.; Lu, G. A review of blast and impact of metallic and sandwich structures. *Electronic Journal of Structural Engineering*, 2007; Volume 1, pp. 92-101.
9. Nton, M. E. *Report submitted to the Honourable Minister Federal Ministry of Solid Minerals Development Abuja*, 2005.
10. Kanchibotla, S. S.; Valery, W.; Morrell, S. Modelling fines in blast fragmentation and its impact on crushing and grinding. In *Explo '99–A conference on rock breaking, The Australasian Institute of Mining and Metallurgy, Kalgoorlie, Australia*, 1999; pp. 137-144.
11. Taiwo, B. O. Effect of charge load proportion and blast controllable factor design on blast fragment size distribution. *Journal of Brilliant Engineering*, 2022; Volume *3*, pp.46-58.
12. Jhanwar, J. C. Theory and practice of air-deck blasting in mines and surface excavations: a review. *Geotechnical and Geological Engineering*, 2011; Volume 5, pp. 651-663.
13. Deniz, V.; Deniz, O. T. The environmental effects of the air shock generated by blasting. *Mugla Journal of Science and Technology*, 2017; Volume 2, pp.166-170.
14. Jethro, M. A., Shehu, S. A., & Kayode, T. S. (2016). Effect of Fragmentation on Loading at Obajana Cement Company Plc, Nigeria. *Int. J. Sci. Eng. Res*, *7*, 608-620.
15. Kinyua, E. M.; Jianhua, Z.; Kasomo, R. M.; Mauti, D.; Mwangangi, J. A review of the influence of blast fragmentation on downstream processing of metal ores. *Minerals Engineering*, 2022; Volume *186*, 107743.
16. Dotto, M. S.; Pourrahimian, Y. Effects of Fragmentation Size Distribution on Truck-Shovel Productivity. *MOL Report Nine*, 2018; pp.335-342.
17. Mackenzie, A. S. Cost of explosive – do you evaluate it properly? *Mining Congress Journal* 1996; pp. 32-41.
18. Kumar, R.; Choudhury, D.; Bhargava, K. Determination of blast-induced ground vibration equations for rocks using mechanical and geological properties. *Journal of Rock Mechanics and Geotechnical Engineering*, 2016; Volume 3, pp.341-349.
19. Choudhary, B. S.; Agrawal, A. Minimization of Blast-Induced Hazards and Efficient Utilization of Blast Energy by Implementing a Novel Stemming Plug System for Eco-Friendly Blasting in Open Pit Mines. *Natural Resources Research*, 2022; *Volume* 6, pp.3393-3410.
20. Hilson, G. Small-scale mining and its socio-economic impact in developing countries. In *Natural Resources Forum*. Oxford, UK and Boston, USA: Blackwell Publishing Ltd, 2002; Vol. 26, No. 1, pp. 3-13.
21. Hilson, G. Small-scale mining in Africa: Tackling pressing environmental problems with improved strategy. *The Journal of Environment & Development*, 2002; Volume 2, pp.149-174.
22. Grobler, H. P. Using electronic detonators to improve all-round blasting performances. *Fragblast*, 2003; Volume 1, pp.1-12.
23. Kalyan, D.; Gopi, B.; Kumar, B. P.; Kumar, B. G.; Raju, G. A study on various surface blast initiation systems. International Research Journal of Engineering and Technology (IRJET), 2021; Vol.ume 7, pp.2616-2618.
24. Matyáš, R.; Pachman, J.; Matyáš, R.; Pachman, J. Introduction to Initiating Substances. *Primary Explosives*, 2013; pp.1-10.
25. Siddiqui, F. I. Measurement of size distribution of blasted rock using digital image processing. *Engineering Sciences*, 2009; *20*(2).
26. Maerz, N. H.; Palangio, T. C.; Franklin, J. A. WipFrag image based granulometry system. In *Measurement of Blast Fragmentation* Routledge, 2018; pp. 91-99.

17

27. Blanco, J. A. S.; Singh, A. K. (Eds.). *Measurement and Analysis of Blast Fragmentation*. CRC Press, 2012.

28. Palangio, T. C.; Maerz, N. H. Case studies using the WipFrag image analysis system. *Fragblast*, 1999; Volume *6*, pp.117-120.

29. Maerz, N. H.; Palangio, T. C.; Franklin, J. A. WipFrag image based granulometry system. In *Measurement of Blast Fragmentation* Routledge, 2018; pp. 91-99.

30. Maerz, N. H.; Palangio, T. C. WipFrag System II–Online Fragmentation Analysis. In *FRAGBLAST 6, Sixth International Symposium for Rock Fragmentation by Blasting*, 1999; pp. 8-12.

31. Faramarzi, F.; Farsangi, M. A. E.; Mansouri, H. Simultaneous investigation of blast induced ground vibration and airblast effects on safety level of structures and human in surface blasting. *International Journal of Mining Science and Technology*, 2014; Volume 5, pp.663-669.

32. Nateghi, R. Evaluation of blast induced ground vibration for minimizing negative effects on surrounding structures. *Soil Dynamics and Earthquake Engineering*, 2012; Volume *43*, pp.133-138.

33. Mutinda, E. K.; Alunda, B. O.; Maina, D. K.; Kasomo, R. M. Prediction of rock fragmentation using the Kuznetsov-Cunningham-Ouchterlony model. *Journal of the Southern African Institute of Mining and Metallurgy*, 2021; Volume 3, pp.107-112.

34. Taiwo, B. O. Improvement of Small-Scale Dolomite Blasting Productivity: Comparison of Existing Empirical Models with Image Analysis Software and Artificial Neural Network Models. *Journal of Mining and Environment*, 2022; Volume 3, pp.627-641.

35. Prasad, S.; Choudhary, B. S.; Mishra, A. K. Effect of stemming to burden ratio and powder factor on blast induced rock fragmentation–a case study. In *IOP conference series: materials science and engineering*, IOP Publishing, 2017; Volume 225, No. 1, p. 012191.

36. Cardu, M.; Giraudi, A.; Oreste, P. A review of the benefits of electronic detonators. *Rem: Revista Escola de Minas*, 2013; Volume *66*, pp. 375-382.

37. Gupta, I. D.; Marwadi, S. C.; Tripathy, G. R.; Shirke, R. R. Environmental Impact of Blasting and Safety of Historic Structures. In *Proceedings of First National Symposium on Environmental Hydraulics, CWPRS Pune* 1992; pp. 26-35.

38. Kahriman, A.; Ozer, U.; Aksoy, M.; Karadogan, A.; Tuncer, G. Environmental impacts of bench blasting at Hisarcik Boron open pit mine in Turkey. *Environmental geology*, 2006; Volume *50*, pp.1015-1023.

39. Vasović, D.; Kostić, S.; Ravilić, M.; Trajković, S. Environmental impact of blasting at Drenovac limestone quarry (Serbia). *Environmental earth sciences*, 2014; Volume *72*, pp.3915-3928.

40. Pantelic, U.; Lilic, P.; Cvjetic, A.; Lilic, N. Environmental Noise Impact Assessment for Large-Scale Surface Mining Operations in Serbia. *Sustainability*, 2023; Volume 3, p. 1798.

41. Nateghi, R. Prediction of ground vibration level induced by blasting at different rock units. International Journal of Rock Mechanics and Mining Sciences, Volume 6, PP. 899-908.

42. Ndibalema, A.; Mine, A. A. G. G. Capturing economic benefits from blasting. In *The Southern African Institute of Mining and Metallurgy: Surface Mining Conference*, 2008; pp. 97-112.

43. Rodríguez Díez, R.; Fernández, P.; Lombardía, C.; Bascompta, M. M. Analysis of blasting vibrations produced In a gold mine using the damage prevention abacus. In Proceedings of the 8th World Congresson Mechanical, Chemical, and Material Engineering (MCM'22). International ASET Inc, 2022.

44. Wang, X., Li, J., Zhao, X., Liang, Y. Propagation characteristics and prediction of blast-induced vibration on closely spaced rock tunnels. Tunnelling and Underground Space Technology, 2022; Volume 123, p.104416.